NASA/TM—2006-213583

Free Body Dynamics of a Spinning Cylinder With Planar Restraint (a.k.a. Barrel of Fun)

Laurentiu Moraru and Florin Dimofte
University of Toledo, Toledo, Ohio

Robert C. Hendricks
Glenn Research Center, Cleveland, Ohio

June 2006

The NASA STI Program Office . . . in Profile

Since its founding, NASA has been dedicated to the advancement of aeronautics and space science. The NASA Scientific and Technical Information (STI) Program Office plays a key part in helping NASA maintain this important role.

The NASA STI Program Office is operated by Langley Research Center, the Lead Center for NASA's scientific and technical information. The NASA STI Program Office provides access to the NASA STI Database, the largest collection of aeronautical and space science STI in the world. The Program Office is also NASA's institutional mechanism for disseminating the results of its research and development activities. These results are published by NASA in the NASA STI Report Series, which includes the following report types:

- TECHNICAL PUBLICATION. Reports of completed research or a major significant phase of research that present the results of NASA programs and include extensive data or theoretical analysis. Includes compilations of significant scientific and technical data and information deemed to be of continuing reference value. NASA's counterpart of peer-reviewed formal professional papers but has less stringent limitations on manuscript length and extent of graphic presentations.

- TECHNICAL MEMORANDUM. Scientific and technical findings that are preliminary or of specialized interest, e.g., quick release reports, working papers, and bibliographies that contain minimal annotation. Does not contain extensive analysis.

- CONTRACTOR REPORT. Scientific and technical findings by NASA-sponsored contractors and grantees.

- CONFERENCE PUBLICATION. Collected papers from scientific and technical conferences, symposia, seminars, or other meetings sponsored or cosponsored by NASA.

- SPECIAL PUBLICATION. Scientific, technical, or historical information from NASA programs, projects, and missions, often concerned with subjects having substantial public interest.

- TECHNICAL TRANSLATION. English-language translations of foreign scientific and technical material pertinent to NASA's mission.

Specialized services that complement the STI Program Office's diverse offerings include creating custom thesauri, building customized databases, organizing and publishing research results . . . even providing videos.

For more information about the NASA STI Program Office, see the following:

- Access the NASA STI Program Home Page at ***http://www.sti.nasa.gov***

- E-mail your question via the Internet to help@sti.nasa.gov

- Fax your question to the NASA Access Help Desk at 301–621–0134

- Telephone the NASA Access Help Desk at 301–621–0390

- Write to:
  NASA Access Help Desk
  NASA Center for AeroSpace Information
  7121 Standard Drive
  Hanover, MD 21076

NASA/TM—2005-213583

Free Body Dynamics of a Spinning Cylinder With Planar Restraint (a.k.a. Barrel of Fun)

Laurentiu Moraru and Florin Dimofte
University of Toledo, Toledo, Ohio

Robert C. Hendricks
Glenn Research Center, Cleveland, Ohio

Prepared for the
Third Biennial International Symposium on Stability Control of Rotating Machinery
(ISCORMA–3)
sponsored by the Bently Pressurized Bearing Company
Cleveland, Ohio, September 19–23, 2005

National Aeronautics and
Space Administration

Glenn Research Center

June 2006

Level of Review: This material has been technically reviewed by technical management.

Available from

NASA Center for Aerospace Information
7121 Standard Drive
Hanover, MD 21076

National Technical Information Service
5285 Port Royal Road
Springfield, VA 22100

Available electronically at http://gltrs.grc.nasa.gov

Free Body Dynamics of a Spinning Cylinder With Planar Restraint (a.k.a Barrel of Fun)

Laurentiu Moraru and Florin Dimofte
University of Toledo
Toledo, Ohio 43606

Robert C. Hendricks
National Aeronautics and Space Administration
Glenn Research Center
Cleveland, Ohio 44135

Summary

The dynamic motion of a cylinder with and without end caps is analyzed based on rotation about its center of mass and restrained by a plane normal to the axis passing through its center of mass at an angle α. For small values of α, the governing equations are simplified, and for symmetric bodies, stability requires rotation greater than $[2\sqrt{(JWL^*)}]/J_X$, where J is the transverse mass moment of inertia, W is the weight of the cylinder, L^* is the cylinder length from the base to the center of mass, and J_X is the mass moment of inertia about the longitudinal axis OX of the barrel. Comparisons to data are made and some applications are discussed.

Introduction

The dynamic motion of a cylinder on a floor or hard plane surface is entertaining and instructive. Many have witnessed the rolling and collapsing motions of a runaway tire, yet the similar behavior of an oil drum is rarely seen. The dynamics of the latter are difficult to describe as the motion can be induced into the drum by a regular periodic change in torque on the periphery of the drum, such as once every time the drum rotates about its transverse axis. The major dilemma resides in its control, which seems to be an accomplishment of those skilled in rhythm and agility. Even though difficult to describe and put into practice, such motions are of interest to rotor dynamicists in stabilizing and maintaining stable spinning spacecraft and in spontaneous unloading of transmissions.

Although the outcome compares favorably with known visual data, we recognize several limitations in that maintenance torques, friction, and other dissipation mechanisms are not completely addressed. The current analysis is not dedicated to the transient period (shown in the video clip which can be viewed in the PDF file of this document at http://gltrs.grc.nasa.gov/reports/2006/TM-2006-213583/TM-2006-213583.pdf). We are mostly concerned with the stability of the barrel after a stationary situation has been reached. Further, while ignored herein, the issues of maintaining control of a large rotating mass are clearly the key, yet can be effectively accomplished with minor periodic adjustments. However, the present report contains only a preliminary analysis of these types of motions. The objective of this analysis is to obtain analytical stability conditions; thus, the model contains inherent approximations and simplifications. Future reports will address different aspects that are not treated herein.

The appendix contains a summary of the formulas that were used to calculate the inertial characteristics of the drum.

Figure 10 illustrates the dynamics and control of a rotating barrel that is set in motion, lifted, and stabilized in spinning about the longitudinal axis via a series of fast and relatively weak impulses applied

by a skilled operator. A video of this motion can be viewed in the PDF file of this document at http://gltrs.grc.nasa.gov

Symbols

A	parameter defined in eq. (28)
A^*	parameter dependent upon sliding conditions
a	constant coefficient in eq. (42)
C_1, C_2	generic notation for integration constants to be determined from initial conditions
c	constant in eq. (42)
D	diameter, m
F_f	friction force
H	height of barrel, m
J	transverse mass moment of inertia, kg m^2
J_X	mass moment of inertia about longitudinal axis OX of barrel, kg m^2
K_0	angular momentum, kg m^2/sec
L	length of barrel, m
L^*	length of cylinder from base to center of mass, m
M	total external moment, Nm
m	mass of disk
N	normal force
R	radius of barrel, m
r	position vector of the acting point of a force, m
t	time, sec
W	weight of cylinder, N
α	nutation angle, deg
η	constant in eq. (44)

θ polar angle in a set of cylindrical coordinates (r, θ, z)

μ friction coefficient

ν precession angle, deg

ξ location of center of mass measured from base upward in fractions (0 to 1) of half of the length of the barrel

ρ density, kg/m^3

σ constant parameter in eq. (42)

σ_s surface element in eq. (56)

τ thickness of metal sheet, m

φ Eulerian rotation

χ geometric parameter ($\equiv L^* \sin \alpha - R \cos \alpha$), m

Ψ dummy parameter, where $\Psi_j \equiv \Psi$ along j-coordinate axis, $\Psi_t \equiv d\Psi/dt$, $\Psi_{tt} \equiv d^2\Psi/dt^2$

ω angular speed, rad/sec

Subscripts:

CG center of gravity

N normal force

p precession

S in R_S represents radius of circle described by the base of the spinning drum

t time derivative

The main geometric elements are indicated in figure 1.

The position of the mass center is $L^* = \xi L/2$, where ξ is the location of the center of mass measured from the base upward (in percentages of half the length L of the barrel).

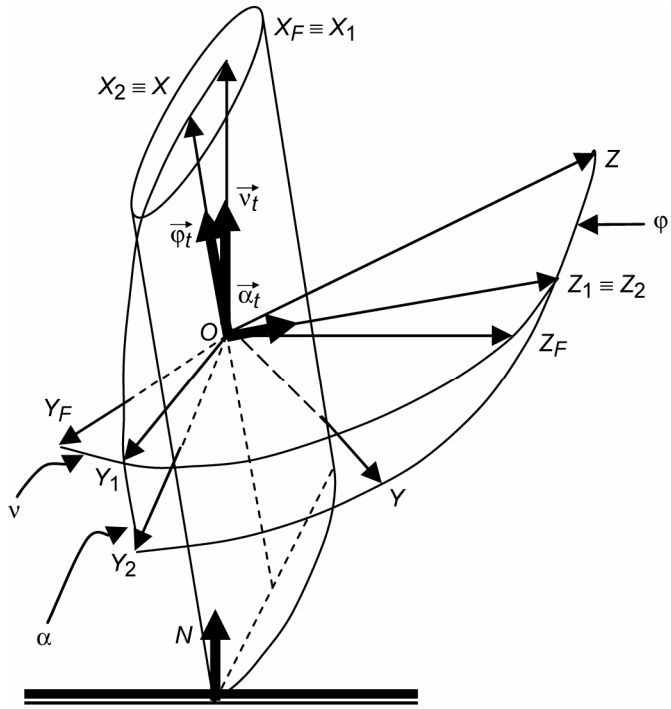

Figure 1.—Position angles and rotations of frames of axes.

Frictionless Analysis

Preliminary Aspects

The dynamics of the cylinder is the same whether the cylinder has closed ends or not. With fixed ends or heads, the cylinder is termed a "drum," without a closed upper end, an "open drum," and without either end closed, a "plain cylinder." In all cases, the restraint is that of a flat surface upon which the cylinder is supported and rotates. To support the motion, the cylinder must spin on multiple axes, and this is the motion analyzed herein.

The dynamic modeling of a body can be done in various ways. The method and the position variables can be selected as desired. The analysis developed herein is governed by the following assumptions:

(1) The drum is modeled as a symmetric rigid body whose center of mass is fixed during the motion and is restrained from below by a plane surface.

(2) The center of mass is located on the centerline of the barrel.

(3) The motion is described by the theorem of the moment of momentum or the angular moment. The equations will be written in the body-fixed frame *OXYZ*.

(4) The frame $OX_FY_FZ_F$ is fixed in space.

(5) The frame *OXYZ* is fixed with respect to the drum and executes all the motions of that drum.

The order of rotations necessary to obtain the *OXYZ* frame from $OX_FY_FZ_F$ is (fig.1)

ν about $OX_F \equiv OX_1$
α about $OZ_1 \equiv OZ_2$
φ about $OX_2 \equiv OX$

which is sometimes schematically written as

$$OX_F Y_F Z_F \xrightarrow[OX_F \equiv OX_1]{v} OX_1 Y_1 Z_1 \xrightarrow[OZ_1 \equiv OZ_2]{\alpha} OX_2 Y_2 Z_2 \xrightarrow[OX_2 \equiv OX]{\varphi} OXYZ$$

The friction is not taken into account in the initial analysis; however, it will be added at a later stage. When the friction is neglected, the only moments that act upon the body are produced by the normal force N exerted by the plane.

The components of the normal force are (fig.2):

$$\begin{aligned} N_X &= W\cos\alpha \\ N_Y &= -W\sin\alpha\cos\varphi \\ N_Z &= W\sin\alpha\sin\varphi \end{aligned} \tag{1}$$

The components of the angular speed along the body-fixed axes $OXYZ$ are (fig.3)

$$\begin{aligned} \omega_X &= \varphi_t + v_t\cos\alpha \\ \omega_Y &= \alpha_t\sin\varphi - v_t\sin\alpha\cos\varphi \\ \omega_Z &= \alpha_t\cos\varphi + v_t\sin\alpha\sin\varphi \end{aligned} \tag{2}$$

and the components of the position vector of the acting point of the normal reaction force r are (figs. 1 and 2)

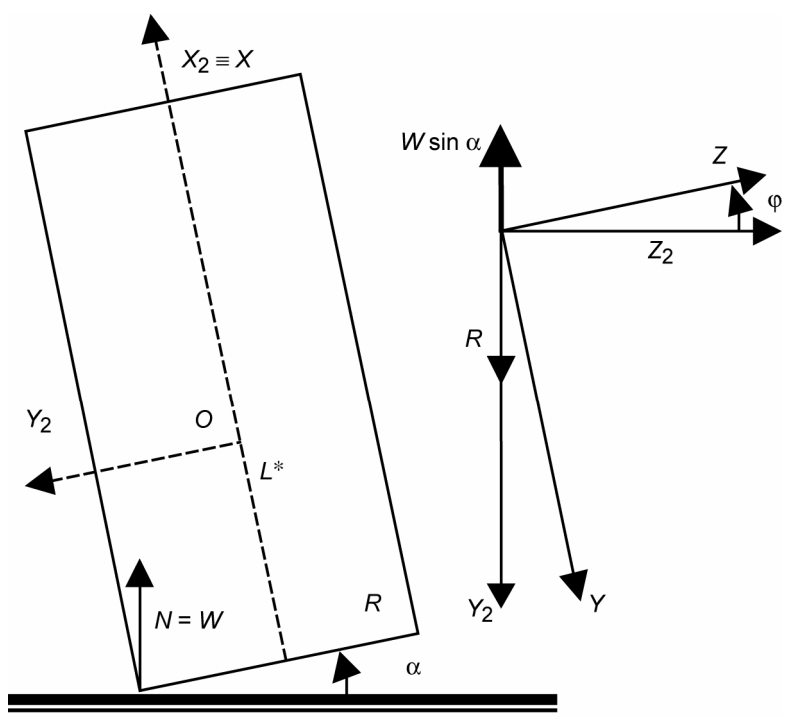

Figure 2.—Force components and position vectors. Friction neglected for case 1.

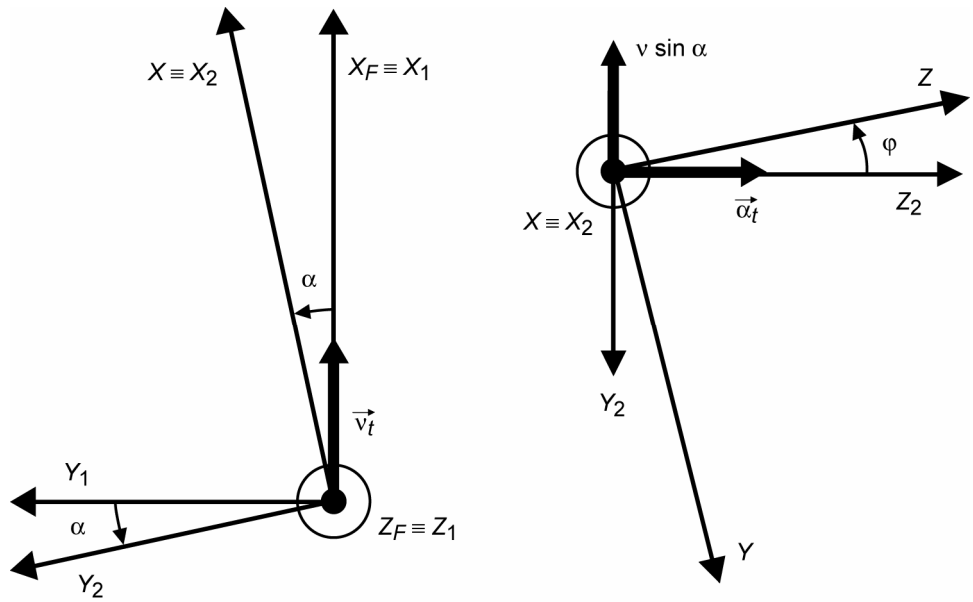

Figure 3.—Components of angular speed.

$$
\begin{aligned}
\left(r_X\right)_N &= \frac{-\xi L}{2} \equiv -L^* \\
\left(r_Y\right)_N &= R\cos\varphi \\
\left(r_Z\right)_N &= -R\sin\varphi
\end{aligned}
\tag{3}
$$

Governing Equations

The moment-of-momentum equations around the fixed-mass center are written in terms of the body axes *OXYZ*:

$$
\left\{\frac{\mathrm{d}\vec{K}_0}{\mathrm{d}t}\right\}_{XYZ} \equiv \left\{\frac{\partial\vec{K}_0}{\partial t} + \vec{\omega}\times\vec{K}_0\right\}_{XYZ} = \left\{\vec{M}\right\}_{XYZ} \tag{4}
$$

When the friction is neglected, the only moments are produced by the normal reaction force

$$
\vec{M} = \vec{r}_N \times \vec{N} = \begin{vmatrix} \vec{i} & \vec{j} & \vec{k} \\ -L^* & R\cos\varphi & -R\sin\varphi \\ W\cos\varphi & -W\sin\alpha\cos\varphi & W\sin\alpha\sin\varphi \end{vmatrix} \tag{5}
$$

so

$$
\begin{aligned}
M_X &= 0 \\
M_Y &= W\sin\varphi\left(L^*\sin\alpha - R\cos\alpha\right) \equiv W\chi\sin\varphi \\
M_Z &= W\cos\varphi\left(L^*\sin\alpha - R\cos\alpha\right) \equiv W\chi\cos\varphi
\end{aligned}
\tag{6}
$$

Next,

$$\vec{K}_0 = \begin{bmatrix} J_X \omega_X & J\omega_Y & J\omega_Z \end{bmatrix}^T \tag{7}$$

and

$$\left\{ \vec{\omega} \times \vec{K}_0 \right\} = \begin{Bmatrix} 0 \\ J_X \omega_X \omega_Z - J\omega_X \omega_Z \\ J\omega_X \omega_Y - J_X \omega_X \omega_Y \end{Bmatrix} \tag{8}$$

Collecting the terms, the *OX* equation is

$$J_X \omega_{Xt} = M_X = 0 \tag{9}$$

So

$$\omega_X = \text{constant} \tag{10}$$

and further

$$\varphi_t = \omega_X - v_t \cos\alpha \tag{11}$$

The *OY* and *OZ* equations are

$$\begin{aligned} J\omega_{Yt} + \left(J_X - J\right)\omega_X \omega_Z &= M_Y \\ J\omega_{Zt} + \left(J - J_X\right)\omega_X \omega_Y &= M_Z \end{aligned} \tag{12}$$

Next,

$$\omega_{Yt} = \alpha_{tt} \sin\varphi + \alpha_t \varphi_t \cos\varphi - v_{tt} \sin\alpha \cos\varphi - v_t \alpha_t \cos\alpha \cos\varphi + v_t \varphi_t \sin\alpha \sin\varphi \tag{13}$$

$$\omega_{Zt} = \alpha_{tt} \cos\varphi - \alpha_t \varphi_t \sin\varphi + v_{tt} \sin\alpha \sin\varphi + v_t \alpha_t \cos\alpha \sin\varphi + v_t \varphi_t \sin\alpha \cos\varphi \tag{14}$$

Next, equation (13) is multiplied by (−cos φ), equation (14) is multiplied by (sin φ), and the expressions are added. Using equations (12) results in

$$\begin{aligned} -\alpha_t \varphi_t + v_{tt} \sin\alpha + v_t \alpha_t \cos\alpha = &-\frac{M_Y}{J} \cos\varphi + \frac{J_X - J}{J} \omega_X \omega_Z \cos\varphi \\ &+ \frac{M_Z}{J} \sin\varphi - \frac{J - J_X}{J} \omega_X \omega_Y \sin\varphi \end{aligned} \tag{15}$$

Using equations (6) and then equations (2) yields

$$-\alpha_t \varphi_t + v_{tt} \sin\alpha + v_t \alpha_t \cos\alpha = \frac{J_X - J}{J} \omega_X \alpha_t \tag{16}$$

For v_t = constant, that is, $v_{tt} = 0$, the above expression becomes

$$-\alpha_t \varphi_t + v_t \alpha_t \cos\alpha = \left(\frac{J_X - J}{J}\right)\omega_X \alpha_t \tag{17}$$

Now, the body in stable dynamic equilibrium executes stable oscillations about the equilibrium position. So α_t is non-zero and it simplifies. Also, φ_t from (11) yields

$$v_t = \frac{J_X \omega_X}{2J\cos\alpha} \tag{18}$$

and further

$$\varphi_t = \omega_X \left(1 - \frac{J_X}{2J}\right) \tag{19}$$

Next, equation (13) is multiplied by (sin φ), equation (14) is multiplied by (cos φ), and the two expressions are added. Further, using equations (12), then equations (6), and finally equations (2) yields

$$\alpha_{tt} + v_t \varphi_t \sin\alpha = \frac{W}{J}\left(L^* \sin\alpha - R\cos\alpha\right) - \frac{J_X - J}{J}\omega_X v_t \sin\alpha \tag{20}$$

From φ_t of (11), the above expression becomes

$$\alpha_{tt} - v_t^2 \sin\alpha\cos\alpha = \frac{W}{J}\left(L^* \sin\alpha - R\cos\alpha\right) - \frac{J_X}{J}\omega_X v_t \sin\alpha \tag{21}$$

and finally, with v_t of (18), the governing equation of the α angle is

$$\alpha_{tt} + \frac{J_X^2}{4J^2}\omega_X^2 \tan\alpha = \frac{W}{J}\left(L^* \sin\alpha - R\cos\alpha\right) \tag{22}$$

For small α, tan α ≅ sin α ≅ α and cos α ≅ 1; thus, the equation becomes a constant coefficients equation:

$$\alpha_{tt} + \left(\frac{J_X^2}{4J^2}\omega_X^2 - \frac{W}{J}L^*\right)\alpha = -\frac{WR}{J} \tag{23}$$

The solution $\alpha = \alpha_{\text{homogeneous}} + \alpha_{\text{particular}}$ is stable when the homogeneous part does not contain exponentials of the form exp(±*rt*), with *r* a real number. So, we need the characteristic equation

$$r^2 + \left(\frac{J_X^2}{4J^2}\omega_X^2 - \frac{W}{J}L^*\right) = 0 \tag{24}$$

to have complex solutions such that

$$\frac{J_X^2}{4J^2}\omega_X^2 - \frac{W}{J}L^* > 0 \tag{25}$$

which yields the stability condition

$$\omega_X > \frac{2\sqrt{WL^*\,J}}{J_X} \tag{26}$$

The analytical solution of equation (23) (for small α angles) can be written as

$$\alpha = -\frac{WR}{JA} + \tilde{\alpha}\sin\left(\sqrt{A}\,t + \varphi\right) \tag{27}$$

where

$$A = \left(\frac{J_X^2\omega_X^2}{4J^2} - \frac{WL^*}{J}\right),\ \tilde{\alpha} = \sqrt{\left(\alpha_0 + \frac{WR}{JA}\right)^2 + \frac{\alpha_{0t}}{A}},\ \text{and}\ \varphi = \tan^{-1}\left[\left(\alpha_0 + \frac{WR}{JA}\right)\frac{\sqrt{A}}{\alpha_{0t}}\right] \tag{28}$$

It can be readily seen that for zero initial conditions ($\alpha_0 = 0$ and $\dot{\alpha}_0 \equiv \alpha_{0t} = 0$) and for $W \to 0$, the motion is not an oscillation and the axis of the body remains oriented toward a fixed position. This is in fact a well-known property of a gyroscope, which is not subject to external influences (also known as Euler gyroscope).

Simplified Analyses

In an alternate, much simpler perspective, just by analyzing the static neutral stability with no slip interface for $\alpha+ = \arctan(2R/h)$ and $R_S \equiv R \sec \alpha+$, if

$$R\frac{\mathrm{d}\varphi}{\mathrm{d}t} = \text{rim speed} = R_S\frac{\mathrm{d}v}{\mathrm{d}t}\ \text{ and if }\ \frac{\mathrm{d}v}{\mathrm{d}t} = \text{constant} \tag{29}$$

and we have pure rolling with no slip, then if α increases, $\mathrm{d}\varphi/\mathrm{d}t$ and R_S increase. Also, if α decreases, both $\mathrm{d}\varphi/\mathrm{d}t$ and R_S decrease.

Also, in an even more simplified analysis, the balance point on the rim of an ideal cylindrical drum, albeit unstable, is at an angle

$$\alpha_b = \tan^{-1}\left(\frac{2R}{H}\right) \tag{30}$$

with an equilibrium rolling radius of

$$R_S = R\sec\alpha_b \tag{31}$$

For a barrel, one may approximate that $H = 0.87$ m and $2R = 0.58$ m. So, α_b is about 0.6 rad and R_S is about $0.8R$. More accurately, $\alpha_b = 0.588$ rad (33.7°) and $R_S = 0.2413$ m

Alternate Approach

No close solution can be found for the general equation of the α angle, and a complete study of the stability can only be done numerically. Many bodies with a gyroscopic motion are generally known to become unstable at high nutation angles, so the small-angle stability condition is usually a good indicator for the stability domain. If a more detailed stability analysis is desired, equation (22) has to be integrated numerically. Figures 4(a) and (b) compare the analytical solution for small α with the numerical solution for a closed drum with a L/D ratio = 1.5 for ω_X three and four times higher than the theoretical stability limit, respectively. Figures 4(c) and (d) are similar to figures 4(a) and (b), but they are obtained using a slightly larger initial angle α_0. Now, the current analysis is not aimed at obtaining a complete equation for the nutation angle. As it was already mentioned in the Introduction, herein we are only concerned with stability. The current modeling is not intended to provide a complete equation that would determine the accurate value of the angle α. The equation obtained herein can only be used as an indication of the stability of the motion. A stable solution of the equation can just indicate a stable behavior of the body, whereas an unstable solution is a warning that the body is unstable.

For the completeness of this report, it is worth recalling that the analytical analysis presented above contains inherent approximations and that an accurate study of the dynamic requires the integration of the full version of the governing equations. The computation of the actual values of the variables requires the use of the angular momentum equations (12) along with the kinematic equations that can be readily obtained by solving equations (2) for φ_t ,α_t, and ν_t.

Figures 4(e) and (f) present results obtained by the integration of the general equations. Here the full system of the governing equations is integrated numerically. The variable ω_X is gradually increased until it reaches a steady-state value equal to three times the critical value determined by equation (26). The nutation angle oscillates steadily around a median position, as shown in figure 4(e). The orbit of the center point of the top lid is shown in figure 4(f). This orbit shows the series of fast small oscillations that are "wrapped" around a circle. To conclude, the analytical model is a good indicator of the stability; however, a complete dynamic analysis requires the full set of equations.

Equation (22) can be integrated using the standard numerical procedures, such as Runge-Kutta or Adams. An alternate solution method can be also considered.

First, let $\alpha_t \equiv \zeta$, and then equation (22) becomes

$$\frac{\zeta\,\mathrm{d}\zeta}{\mathrm{d}\alpha} + a_1 \tan\alpha = a_2 \sin\alpha - a_3 \cos\alpha \tag{32}$$

where $a_1 = [(J_X^2/(4J^2)]\,\omega_X^2$, $a_2 = (W/J)\,(\xi L/2)$, and $a_3 = (W/J)R$.

Next,

$$\frac{1}{2}\zeta^2 - a_1 \ln\left(\cos\alpha\right) = -a_2 \cos\alpha - a_3 \sin\alpha + C_1 \tag{33}$$

so

$$\frac{\mathrm{d}\alpha}{\mathrm{d}t} = \left[a_1 \ln\left(\cos\alpha\right) - a_2 \cos\alpha - a_3 \sin\alpha + C_1\right]^{1/2} \tag{34}$$

and

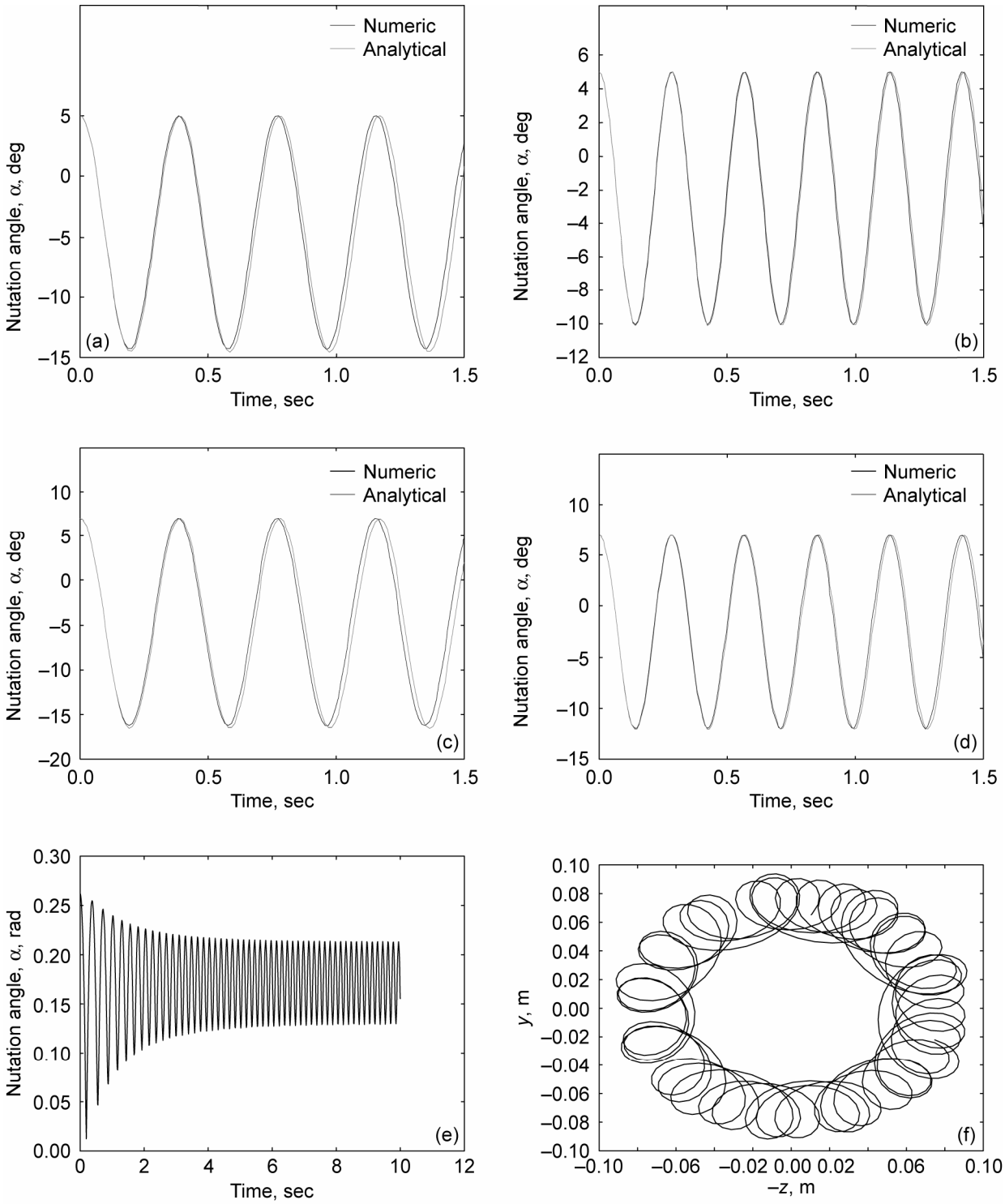

Figure 4.—Analytical and numerical solutions. (a) Speed, $\omega_X = 3^*[2\sqrt{(JWL^*)}]/J_x$. (b) Speed, $\omega_X = 4^*[2\sqrt{(JWL^*)}]/J_x$. (c) Speed, $\omega_X = 3^*[2\sqrt{(JWL^*)}]/J_x$. (d) Speed, $\omega_X = 4^*[2\sqrt{(JWL^*)}]/J_x$. (e) Complete model integration; speed, $(\omega_X)_{steady} = 3^*[2\sqrt{(JWL^*)}]/J_x$. (f) Complete model integration; orbit of center of top lid (top view); speed, $(\omega_X)_{steady} = 3^*[2\sqrt{(JWL^*)}]/J_x$.

$$t = C_2 + \int \left[a_1 \ln(\cos\alpha) - a_2 \cos\alpha - a_3 \sin\alpha + C_1 \right]^{-1/2} \mathrm{d}\alpha \tag{35}$$

Next, let $\zeta = \cos\alpha$ to yield

$$t = C_2 - \int \left[C_1 + a_1 \ln\zeta - a_2\zeta - a_3\left(1-\zeta^2\right)^{1/2} \right]^{-1/2} \left(1-\zeta^2\right)^{-1/2} \mathrm{d}\zeta \tag{36}$$

Again, the expressions have to be computed numerically.

Applications (Computations for Barrels)

Several applications are presented for the cases of an open barrel, a completely closed barrel, and a barrel with the bottom lid closed and the top lid removed. The typical barrel was 0.58 m in diameter, 0.87 m in height, and had a metal thickness of 1.01 mm. The density of the steel was 7753 kg/m^3, so the weight of the closed drum was 163.3 N. For this drum, the *L*/*D* ratio was 1.5. The mass and inertia moments are presented in the appendix. We considered other cases for *L*/*D* ratios of 1 and 2. The results are summarized in table I.

TABLE I.—THEORETICAL STABILITY LIMITS
[Diameter, *D*, 0.58 m; minimum stable speed, ω_X, rad/sec.]

	For length-diameter ratios *L*/*D* of—					
	1.0		1.5		2.0	
	ω_X, rad/sec	*W*, N[a]	ω_X, rad/sec	*W*, N[a]	ω_X, rad/sec	*W*, N[a]
Drum	1.38	122.5	20.3	163.3	27.8	204.1
Open drum	10.8	102	16.7	142.9	23.5	183.7
Plain cylinder (shell, no ends)	10.6	81.6	15.9	122.5	22.3	163.3
Static angle α_b, deg	45	45	33.7	33.7	26.6	26.6
Equilibrium R_S, m	0.41	0.41	0.35	0.35	0.32	0.32

[a]1 Newton = 0.224808943 $\mathrm{lb_f}$

Effect of Friction

Two types of friction act upon the drum: rolling friction is perpendicular to the OY_2 axes and opposes the precession of the drum; sliding friction is parallel to the OY_2 axes and opposes the increase of the nutation angle α (fig.5). The rolling friction is much smaller than the sliding friction, so in the subsequent analysis is neglected (in industrial gyroscopic applications this is usually compensated by an electric motor).

The components of the sliding friction force are

$$\begin{aligned} F_{fX} &= F_f \sin\alpha \\ F_{fY} &= F_f \cos\alpha\cos\varphi \\ F_{fZ} &= -F_f \cos\alpha\sin\varphi \end{aligned} \tag{37}$$

and the friction force is applied in the same point as the normal *N*. Following the same development as before, the equation for the angle α becomes

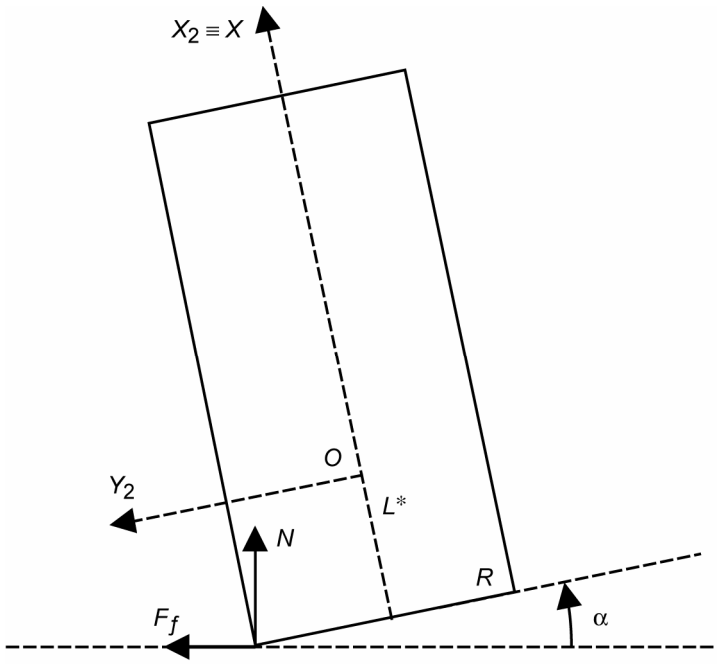

Figure 5.—Forced components. Sliding friction included for case 2.

$$\alpha_{tt} + \frac{J_X^2 \omega_X^2}{4J^2} \tan\alpha = \frac{W}{J}\left(L^* \sin\alpha - R\cos\alpha\right) - \frac{F_f}{J}\left(L^* \cos\alpha + R\sin\alpha\right) \tag{38}$$

and for small angles,

$$\alpha_{tt} + \frac{J_X^2 \omega_X^2}{4J^2}\alpha = \left(\frac{WL^*}{J} - \frac{F_f R}{J}\right)\alpha - \frac{WR}{J} - \frac{F_f L^*}{J} \tag{39}$$

In a general case, the friction force can be written as

$$F_f = \mu N + A^* \alpha_t \tag{40}$$

where μ is the coefficient of friction and A^* depends upon the sliding conditions. So

$$\alpha_{tt} + \left(\frac{J_X^2}{4J^2}\omega_X^2 - \frac{WL^*}{J} + \frac{F_f R}{J}\right)\alpha = -\frac{WR}{J} - \frac{\mu N L^*}{J} - \frac{A^* L^* \alpha_t}{J} \tag{41}$$

where μ is the friction coefficient.

Now, the friction force in the left-hand-side term is usually much smaller than the other terms, so it will be neglected. As a consequence, the stability condition does not change and the equation can be written as

$$\alpha_{tt} + a\alpha_t + \omega_p^2 \sigma\alpha = c \tag{42}$$

where the constants a, c, σ, and ω_p can be readily identified by inspection. For example,

$$\omega_p^2 \equiv v_t^2 = \frac{J_X^2 \omega_X^2}{4J^2} \text{ and } \sigma = 1 - \frac{WL^*}{J\omega_p^2} \tag{43}$$

The solution is

$$\alpha = C_1 \left[\exp\left(\frac{-at}{2} \right) \right] \sin\left(\omega_p \sqrt{\eta\sigma}\, t + C_2 \right) + \frac{c}{\omega_p^2 \sigma} \tag{44}$$

where C_1 and C_2 are integration constants to be determined from the initial conditions and $\eta = a^2/\left(4\omega_p^2\sigma\right) - 1$.

It can now be readily seen that for $a > 0$, the oscillatory component decreases rapidly and the solution may appear to be a constant equal to the particular solution of the nonhomogeneous equation; that is,

$$\alpha \cong \frac{c}{\omega_p^2 \sigma} \tag{45}$$

However, the result provided by equation (27) may not be the correct steady-state value. The correct steady-state value can only be obtained by integrating equations (2), (4), and (5).

Additional Applications

The foregoing treatment of the barrel follows general methodologies that are usually applied for gyroscopic motions. Other different applications can be found in various sources. Maybe the most simple and the most intuitive is the steady precession of a symmetric gyroscope or top (fig. 6). The motion is described as shown in the Governing Equations section; however, here the angular momentum theorem is written with respect to the contact point. Again, in a first approximation, the effects of the friction may be neglected, so the only moments that act upon the body are produced by the weight.

The components of the load are

$$\begin{aligned} W_X &= -W \cos\alpha \\ W_Y &= W \sin\alpha \cos\varphi \\ W_Z &= -W \sin\alpha \sin\varphi \end{aligned} \tag{46}$$

and the coordinates of the mass center are

$$\begin{aligned} \left(r_X\right)_W &= L^* \\ \left(r_Y\right)_W &= L^* \sin\alpha \cos\varphi \\ \left(r_Z\right)_W &= -L^* \sin\alpha \sin\varphi \end{aligned} \tag{47}$$

So again,

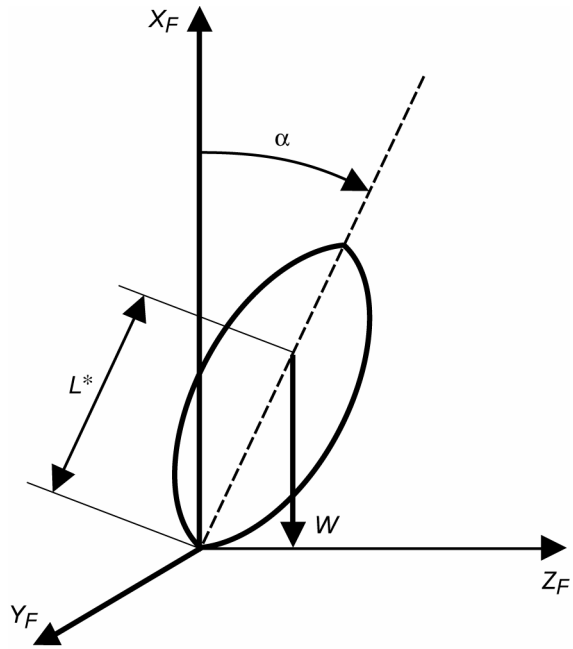

Figure 6.—Steady precession of symmetric top.

$$
\begin{aligned}
M_X &= 0 \\
M_Y &= WL^* \sin\alpha\left(1+\cos\alpha\right)\sin\varphi \\
M_Z &= WL^* \sin\alpha\left(1+\cos\alpha\right)\cos\varphi
\end{aligned}
\tag{48}
$$

Following the same procedures as before would yield

$$
a_{tt} + \left(\frac{J_X^2}{4J^2}\right)\omega_X^2 \tan\alpha = \frac{W}{J}\left[L^* \sin\alpha\left(1+\cos\alpha\right)\right] \tag{49}
$$

which for small α becomes

$$
a_{tt} + \left(\frac{J_X^2}{4J^2}\omega_X^2 - \frac{2W}{J}L^*\right) = 0 \tag{50}
$$

and again, the motion is stable if

$$
\omega_X > 2\left[\frac{\left(2JWL^*\right)^{1/2}}{J_X}\right] \tag{51}
$$

where J is now computed with respect to the support point.

As it is generally known from the top experiments, a decrease in the angular speed produces an increase in the α angle and finally the top falls on the table. It is also known that if the angle α increases above a certain limit, the motion destabilizes, an effect that is more important at low speeds.

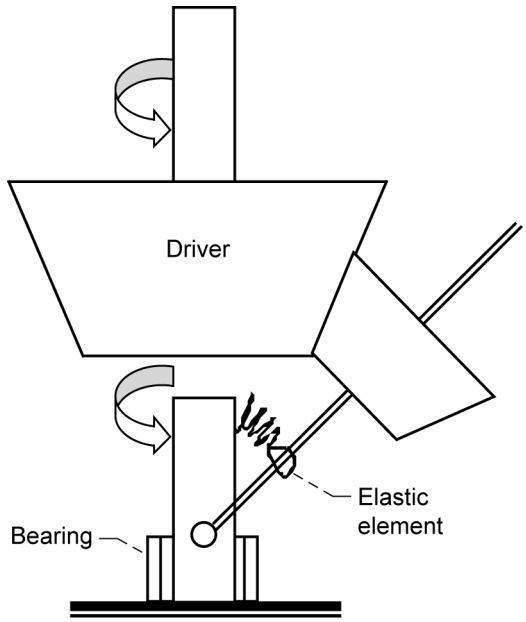

Figure 7.—Bevel gear assembly.

The same type of analysis may also apply for certain types of bevel gears (fig. 7). When the driver gear is lifted, the driven shaft moves around the fixed point (the joint). Here the analysis would somehow be different because of the influence of the elastic element. The driven shaft is also subject to the influence of a hydrodynamic force due to the fluid film in the joint.

The study of the motion of bodies with various restraints is an important part of dynamics, and different aspects are widely treated in various textbooks on gyroscopes, dynamics of mechanism, flight dynamics, rotordynamics, and so on. Closed-form solutions can be found for simplified cases and analytical stability considerations can sometimes be deduced. A full review of the analytical solutions is way beyond the scope of this paper. However, as an example, we will provide two more results that appear in the plain restrained motion of a thin disk.

Figure 8 illustrates the first example, the rolling of a disk with the disk plane nearly vertical ($\alpha \approx 90°$). It can be proven (ref. 1) that the disk oscillates around the vertical plane when the spin is larger than

$$\omega_X^2 > \frac{WJR}{J + mR^2} \tag{52}$$

where R is the radius of the disk and m is the mass. As indicated in the appendix, the mass moments of inertia are $J_X = mR^2/2$ and $J = mR^2/4$. The stability condition (eq. (52)) is applicable for cylinders where the radius is much larger than the height. The classical example of this motion is a coin rolling along a table.

Also, when the disk spins upright (fig. 9), it can be proven (ref. 1) that the spinning motion is stable as long as

$$v_t^2 = \dot{v}^2 > \frac{WRJ}{J + mR^2} \tag{53}$$

The expression of the transverse moment of inertia J has just been indicated above. An example of this motion is the classical spinning of a penny or silver dollar on a table top.

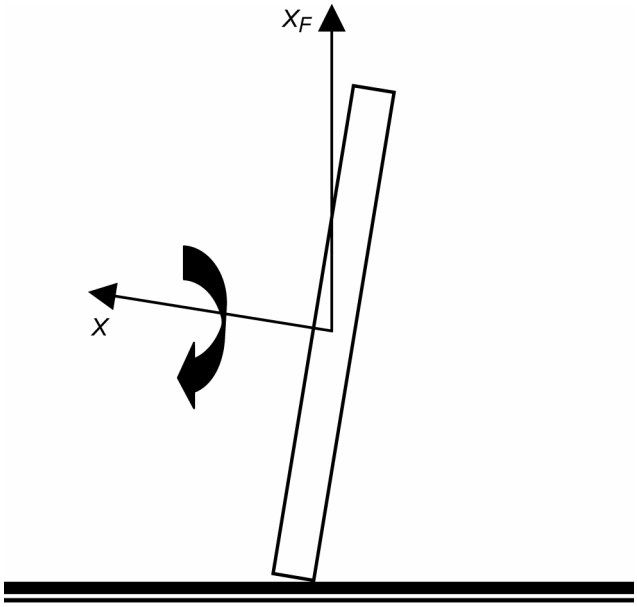

Figure 8.—Disk rolling nearly vertical.

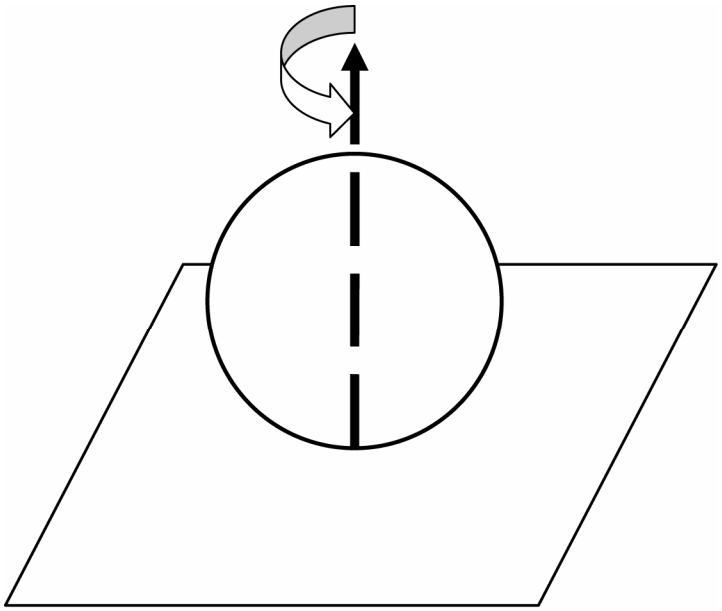

Figure 9.—Upright spinning of disk.

Video Clip

The video illustrates the skill of a street merchant walking his empty, open-end, 55-gal drum about a heavily trafficked street with nearly perfect control as one might walk a dog. The drum motion and feedback control are maintained by a cadence of regular hand-imparted surface torques at each rotation of the barrel. Small angles from vertical require short slaps and large angles require complex upward motions of the hand and body. Figure 10 presents some still shots taken in the transient period during the lifting of the barrel. A video of this motion can be viewed in the PDF file of this document on the web at http://gltrs.grc.nasa.gov/reports/2006/TM-2006-213583/TM-2006-213583.pdf

Click here to play movie

(a)

(b)

Figure 10.—(a) Video clip illustrating the dynamics and control of a rotating barrel. (b) Lifting the barrel (motion of barrel during transient stage).

Conclusions

The dynamic motions of a drum about its center of mass that is restrained by a plane normal to the axis of rotation passing through its center of mass at nutation angle α are both entertaining and instructive. Yet, once spinning, the motion of the drum can be controlled by regular periodic changes in torque on the periphery of the drum, such as once every time the drum rotates. This report presents a preliminary analysis of these types of motions. A model is deduced using the theorem of the moment of momentum. The governing equations for the nutation angle are deduced. For small values of α, the governing equations are simplified and for the illustration, control seems to be an accomplishment of those skilled in rhythm and agility. The drum can be stabilized provided that $\omega_X > 2\left[\left(JWL^*\right)^{1/2} / J_X\right]$, where ω_x is the minimum stable speed, J is the transverse mass moment of inertia, W is the weight of the cylinder, L^* is the distance from the base to the center of mass, and J_X is the mass moment of inertia about the longitudinal axis OX of the barrel.

For the open drum or barrel of the illustration, assuming constant material thicknesses, that rotation speed is calculated to be

$$\omega_X > 16.7 \text{ rad/sec with open-drum weight of 143 N and } L/D = 1.5 \tag{54}$$

$$\omega_X > 10.8 \text{ rad/sec with open-drum weight of 102 N and } L/D = 1 \tag{55}$$

For the open drum of the illustration, the rotating speed was between 1 and 3 rotations/sec or (6.3 and 18.8 rad/sec) depending on angle α.

Appendix—Moments of Inertia

Details of Calculations of Mass Moments of Inertia

The expressions of the inertia moments can be found in various engineering handbooks. Some expressions are presented in the body of this work for completeness. The geometric elements are shown in figure 11.

For the plain cylinder or shell,

$$Jx_s = \int_{\Omega} \left(y^2 + z^2\right) \mathrm{d}m = \rho \int_{\Omega} \left(y^2 + z^2\right) \mathrm{d}V = \rho\tau \int_{\Sigma} \left(y^2 + z^2\right) \mathrm{d}\sigma_s \tag{56}$$

where $\mathrm{d}\sigma_s = r\mathrm{d}\theta\mathrm{d}x$, $y = r \sin\theta$, and $x = r\cos\theta$, so

$$Jx_s = \rho\tau \int_0^{2\pi} \int_{-h}^{L-h} r^3 \,\mathrm{d}\theta\,\mathrm{d}x = 2\pi\rho\tau r^3 L = 2\pi\rho\tau r L r^2 = m_1 r^2 \tag{57}$$

Next,

$$Jy_s = \rho\tau \int_{\Sigma} \left(x^2 + z^2\right) \mathrm{d}\sigma_s = \rho\tau r_1 \int_0^{2\pi} \int_{-h}^{L-h} \left(x^2 + r_1^2 \cos^2\theta\right) \mathrm{d}\theta\,\mathrm{d}x = 2\pi\rho\tau r_1 \int_{-h}^{L-h} \left(x^2 + \frac{r_1^2}{2}\right) \mathrm{d}x \tag{58}$$

where $\cos^2\theta = (\cos 2\theta + 1)/2$ and $r_1 = (R_{OD} + R_{ID})/2 \approx R$, so

$$Jy_s = 2\pi\rho\tau r_1 L \left[\left(\frac{x^3}{3L}\right) + \left(\frac{r_1^2 x}{2L}\right)\right]_{-h}^{L-h} = m_1 \left[\left(\frac{L^2 - 3Lh + 3h^2}{3}\right) + \left(\frac{R^2}{2}\right)\right] \tag{59}$$

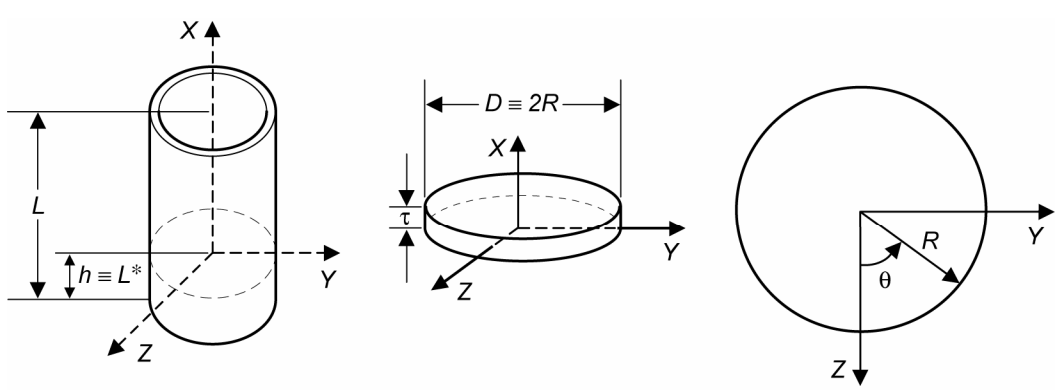

Figure 11.—Geometric elements.

For $h \equiv L^* = \xi L/2$, where $h \equiv L^*$ and $\xi = m_1/(m_1 + m_2)$ are measured from the base,

$$Jy_s = m_1 \left\{ \left[L^2 \left(\frac{4 - 6\xi + 3\xi^2}{12} \right) \right] + \left(\frac{R^2}{2} \right) \right\} \tag{60}$$

and for $\xi = 1$,

$$Jy_s = m_1 \left[\left(\frac{L^2}{12} \right) + \left(\frac{R^2}{2} \right) \right] \tag{61}$$

For end caps or bases,

$$Jx_b = \rho\tau \int_{\Sigma} \left(y^2 + z^2 \right) \mathrm{d}\sigma_b = \rho\tau \int_0^R \int_0^{2\pi} r^3 \, \mathrm{d}r \, \mathrm{d}\theta = \left(\frac{\pi\rho\tau R^2 R^2}{2} \right) = \left(\frac{m_2 R^2}{2} \right) \tag{62}$$

$$Jy_b = \rho\tau \int_{\Sigma} \left(x^2 + z^2 \right) \mathrm{d}\sigma_b \rightarrow \rho\tau \int_{\Sigma} z^2 \, \mathrm{d}\sigma_b = \rho\tau \int_0^R \int_0^{2\pi} r^3 \, \mathrm{d}r \cos^2\theta \, \mathrm{d}\theta = \left(\frac{\pi\rho\tau R^2 R^2}{4} \right) = \left(\frac{m_2 R^2}{4} \right) \tag{63}$$

So, for the plain cylinder,

$$Jx_s = m_1 R^2 \tag{64}$$

and

$$Jy_s = m_1 \left[L^2 \left(\frac{4 - 6\xi + 3\xi^2}{12} \right) \right] + \left(\frac{R^2}{2} \right) \tag{65}$$

and for $\xi = 1$, the geometric center and mass center coincide:

$$Jy_s = m_1 \left[\left(\frac{L^2}{12} \right) + \left(\frac{R^2}{2} \right) \right] \tag{66}$$

For the open drum or cylinder plus the base (or end cap),

$$Jx = Jx_s + Jx_b = m_1 R^2 + \frac{m_2 R^2}{2} = m_1 R^2 \left(\frac{1 + m_2}{2 m_1} \right) \tag{67}$$

and

$$
\begin{aligned}
Jy &= Jy_s + m_1\left(\frac{\xi^* L}{2}\right)^2 + Jy_b + m_2\left[\left(\frac{L}{2}-\frac{\xi^* L}{2}\right)^2\right] \\
&= m_1\left\{\left[\left(\frac{L^2}{12}\right)+\left(\frac{R^2}{2}\right)\right]+\left(\frac{\xi^* L}{2}\right)^2\right\} + m_2\left\{\frac{R^2}{4}+\left[\frac{\left(1-\xi^*\right)L}{2}\right]^2\right\} \\
&= \left(\frac{m_1 L^2}{2}\right)\left(\left\{\left[\left(\frac{1}{6}\right)+\left(\frac{R}{L}\right)^2\right]+\frac{\xi^{*2}}{2}\right\}+\left(\frac{m_2}{m_1}\right)\left[\frac{\left(\frac{R}{L}\right)^2}{2}+\frac{\left(1-\xi^*\right)^2}{2}\right]\right) \\
&= \left(\frac{m_1 L^2}{4}\right)\left\{\left(\frac{1}{3}\right)+2\left(\frac{R}{L}\right)^2+\left(\frac{m_2}{m_1}\right)\left[\left(\frac{R}{L}\right)^2+\left(1-\xi^*\right)^2\right]+\xi^{*2}\right\}
\end{aligned}
\tag{68}
$$

where, from the moment balance in static equilibrium, $\xi^* = m_2/(m_1 + m_2)$ and $\xi = m_1/(m_1 + m_2)$.

For the drum or barrel or cylinder with the same ends,

$$
Jx = Jx_s + Jx_b + Jx_b = m_1 R^2\left[1+\left(\frac{m_2}{m_1}\right)\right] \tag{69}
$$

and

$$
\begin{aligned}
Jy &= Jy_s + 2\left[Jy_b + m_2\left(\frac{L}{2}\right)^2\right] = m_1\left[\left(\frac{L^2}{12}\right)+\left(\frac{R^2}{2}\right)\right]+m_2\left[\frac{\left(R^2+L^2\right)}{2}\right] \\
&= \left(\frac{m_1 L^2}{2}\right)\left\{\left[\left(\frac{1}{6}\right)+\left(\frac{R}{L}\right)^2\right]+\left(\frac{m_2}{m_1}\right)\left[1+\left(\frac{R}{L}\right)^2\right]\right\} \\
&= \left(\frac{m_1 L^2}{2}\right)\left\{\left(\frac{1}{6}\right)+\left(\frac{m_2}{m_1}\right)+\left(\frac{R}{L}\right)^2\left[1+\left(\frac{m_2}{m_1}\right)\right]\right\}
\end{aligned}
\tag{70}
$$

Main Formulations of Mass Moments of Inertia

For the plain cylinder or for the shell (symmetric),

$$
\left(J_{Xs}\right)_{CG} = m_1 R^2 \quad \text{and} \quad \left(J_s\right)_{CG} = \left(\frac{m_1 L^2}{2}\right)\left[\left(\frac{1}{6}\right)+\left(\frac{R}{L}\right)^2\right] \tag{71}
$$

For the open drum (shell plus end cap, asymmetric),

$$\left(J_X\right)_{CG^*} = \left(J_{Xs}\right)_{CG} + \left(J_{Xb}\right)_{CG} = m_1 R^2 \left(1 + \frac{0.5 m_2}{m_1}\right) \tag{72}$$

and

$$\begin{aligned}\left(J\right)_{CG^*} &= \left(J_s\right)_{CG} + m_1\left(\frac{\xi^* L}{2}\right)^2 + \left(J_b\right)_{CG} + m_2\left[\left(1-\xi^*\right)\frac{L}{2}\right]^2 \\ &= \left(\frac{m_1 L^2}{4}\right)\left\{\left(\frac{1}{3}\right) + 2\left(\frac{R}{L}\right)^2 + \left(\frac{m_2}{m_1}\right)\left[\left(\frac{R}{L}\right)^2 + \left(1-\xi^*\right)^2\right] + \xi^{*2}\right\}\end{aligned} \tag{73}$$

The location of the center of gravity of the open drum (CG^*) from the center of gravity of the shell (CG_{shell}) is defined by

$$\xi^* = \frac{m_2}{\left(m_1 + m_2\right)} \tag{74}$$

For the closed drum (shell plus both ends capped, symmetrical),

$$\left(J_X\right)_{CG} = \left(J_{Xs}\right)_{CG} + 2\left(J_{Xb}\right)_{CG} = m_1 R^2\left[1 + \left(\frac{m_2}{m_1}\right)\right] \tag{75}$$

and

$$\left(J_s\right)_{CG} = \left(\frac{m_1 L^2}{2}\right)\left\{\left(\frac{1}{6}\right) + \left(\frac{m_2}{m_1}\right) + \left(\frac{R}{L}\right)^2\left[1 + \left(\frac{m_2}{m_1}\right)\right]\right\} \tag{76}$$

The inertial properties of the typical barrel (L = 0.87 m and D = 0.58 m) are given in table II.

TABLE II.—INERTIA DATA OF BARREL
[Length, L, 0.87 m; diameter, D, 0.58 m.]

Geometry	Mass moment of inertia about longitudinal axis of barrel, J_X, kg m^2	Transverse mass moment of inertia, J, kg m^2	Weight of cylinder, W, N
Drum	1.225	2.187	163.3
Open drum	1.138	1.694	142.9
Plain cylinder (shell, no ends)	1.050	1.313	122.5

Reference

1. Thomson, W.T.: Introduction to Space Dynamics, John Wiley and Sons, Inc., New York, London, 1963.

REPORT DOCUMENTATION PAGE

Form Approved
OMB No. 0704-0188

Public reporting burden for this collection of information is estimated to average 1 hour per response, including the time for reviewing instructions, searching existing data sources, gathering and maintaining the data needed, and completing and reviewing the collection of information. Send comments regarding this burden estimate or any other aspect of this collection of information, including suggestions for reducing this burden, to Washington Headquarters Services, Directorate for Information Operations and Reports, 1215 Jefferson Davis Highway, Suite 1204, Arlington, VA 22202-4302, and to the Office of Management and Budget, Paperwork Reduction Project (0704-0188), Washington, DC 20503.

1. AGENCY USE ONLY (*Leave blank*)

2. REPORT DATE
June 2006

3. REPORT TYPE AND DATES COVERED
Technical Memorandum

4. TITLE AND SUBTITLE
Free Body Dynamics of a Spinning Cylinder With Planar Restraint
(a.k.a. Barrel of Fun)

5. FUNDING NUMBERS
Cost Center 2250000013

6. AUTHOR(S)
Laurentiu Moraru, Florin Dimofte, and Robert C. Hendricks

7. PERFORMING ORGANIZATION NAME(S) AND ADDRESS(ES)
National Aeronautics and Space Administration
John H. Glenn Research Center at Lewis Field
Cleveland, Ohio 44135–3191

8. PERFORMING ORGANIZATION REPORT NUMBER
E–15050

9. SPONSORING/MONITORING AGENCY NAME(S) AND ADDRESS(ES)
National Aeronautics and Space Administration
Washington, DC 20546–0001

10. SPONSORING/MONITORING AGENCY REPORT NUMBER
NASA TM—2006-213583

11. SUPPLEMENTARY NOTES
Prepared for the Third Biennial International Symposium on Stability Control of Rotating Machinery (ISCORMA–3) sponsored by the Bently Pressurized Bearing Company, Cleveland, Ohio, September 19–23, 2005. Laurentiu Moraru and Florin Dimofte, Department of Mechanical Engineering, University of Toledo, Toledo, Ohio 43606–3390; and Robert C. Hendricks, NASA Glenn Research Center. Responsible person, Robert C. Hendricks, organization code R, 216–977–7507. A link to view the video clip can be found in figure 10 in the online PDF version.

12a. DISTRIBUTION/AVAILABILITY STATEMENT
Unclassified - Unlimited
Subject Categories: 37, 39, and 70
Available electronically at http://gltrs.grc.nasa.gov
This publication is available from the NASA Center for AeroSpace Information, 301–621–0390.

12b. DISTRIBUTION CODE

13. ABSTRACT ***(Maximum 200 words)***

The dynamic motion of a cylinder on a floor or hard surface is both entertaining and instructive. With maintenance torques, motion can be sustained and controlled as illustrated in a video clip that can be viewed in the PDF file of this document. The analysis of such a cylinder with and without end caps is burned on rotation about its center of mass and restrained by a plane normal to the axis passing through its center of mass at an angle α. For small values of α, the governing equations are simplified, and for symmetric bodies, stability requires rotation greater than $[2\sqrt{(JWL^*)}]/J_X$, where J is the transverse mass moment of inertia, W is the weight of the cylinder, L^* is the cylinder length from the base to the center of mass, and J_X is the mass moment of inertia about the longitudinal axis OX of the barrel. Comparisons to data are made and some applications are discussed.

14. SUBJECT TERMS
Rotordynamics; Stability; Spinning Cylinder

15. NUMBER OF PAGES
30

16. PRICE CODE

17. SECURITY CLASSIFICATION OF REPORT	18. SECURITY CLASSIFICATION OF THIS PAGE	19. SECURITY CLASSIFICATION OF ABSTRACT	20. LIMITATION OF ABSTRACT
Unclassified	Unclassified	Unclassified	